

# Design a Digital Electronic Load Controller for Micro-Hydroelectric System Applications

Chong Yee Ming, Martin Anyi, Lakshmanan Gurusamy



**Abstract:** A micro-hydroelectric system is an important alternative for rural electrification, but its output voltage fluctuates over a small change of consumer loads. In order to protect the users and their appliances, the output voltage must be regulated to the nominal voltage of the appliances. For that purpose, this paper describes the concept of a simple and cost effective digital Electronic Load Controller (ELC). The formulation of proportional-integral-derivative (PID) control based ELC algorithm is presented, and the flow chart of the algorithm is derived. The hardware implementation of the ELC was established to verify the concept. By using a laboratory setup, the tuning effect of PID time interval on the voltage regulation was investigated and presented as there is no well documented information about the setting of that variable in literature. The experimental results showed that the ELC performed better with minimum value of time interval. The ELC was also tested with load variations, and the results showed that the output voltage was kept regulated at the nominal voltage despite the load variations. This has confirmed that the concept and methods used in the ELC design proposed in this paper can be considered for the voltage regulation of the micro-hydroelectric system.

**Keywords :** electronic load controller, micro-hydroelectric, voltage regulation, proportional-integral-derivative control.

## I. INTRODUCTION

Providing energy to rural areas without commercial power supply by utility board has given rise to the development of standalone micro-hydroelectric system solutions to provide power. A micro-hydroelectric system is a small-scale power generation system with a power generating capacity ranged from 5kW to 100kW [1], [2]. However, such system has a critical problem in that the output voltage is sensitive to load variation. This is due to the load characteristic of electrical generator, as illustrated in Fig. 1. A generator can produce a nominal voltage (e.g. 240V) when it spins at rated speed (e.g. 1500rpm) under no load condition (0% load). As the load increases from zero to full load (100% load), speed and hence voltage drops below their standard values.

Revised Manuscript Received on January 30, 2020.

\* Correspondence Author

**Chong Yee Ming\***, Department of Electrical and Electronic Engineering, Faculty of Engineering, Universiti Malaysia Sarawak, Kota Samarahan, Malaysia.

**Martin Anyi**, Department of Electrical and Electronic Engineering, Faculty of Engineering, Universiti Malaysia Sarawak, Kota Samarahan, Malaysia.

**Lakshmanan Gurusamy**, Department of Electrical and Electronic Engineering, Faculty of Engineering, Universiti Malaysia Sarawak, Kota Samarahan, Malaysia.

© The Authors. Published by Blue Eyes Intelligence Engineering and Sciences Publication (BEIESP). This is an [open access](https://creativecommons.org/licenses/by-nc-nd/4.0/) article under the CC-BY-NC-ND license <http://creativecommons.org/licenses/by-nc-nd/4.0/>

So, the speed must be first increased above its rated value in order to obtain nominal voltage at 100% load. However, the load utilization by consumers is inconsistent throughout the day.

Consequently, any loss of consumer load will cause the speed and voltage to increase, and this may cause overvoltage and damage to consumer appliances [3].

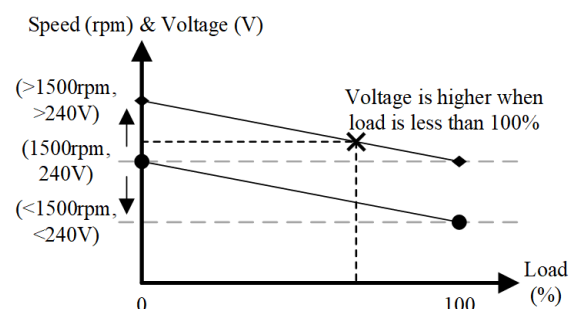


Fig. 1. Load characteristic of generator.

Thus, an ELC is designed to maintain the nominal voltage by keeping full load on the generator. It recovers the loss of total load by absorbing the excess power from a disconnected consumer load with an external load (also called dump load). In contrast, it releases the power from the dump load when a consumer load is connected.

Digital control based ELCs are more compact, cost effective, and reliable as compared to those with analogue controls [4,] [5]. The digital controls in ELCs have been realized by using digital signal processors (DSPs) [6]-[15] and programmable logic controllers (PLCs) [16]. DSPs have intensive computational powers for executing complex algorithms. However, a simple control scheme should be preferred for rural application, and it can be achieved more economically using a microcontroller, which is developed specifically for general purpose application. Meanwhile, PLCs only operate in discrete logical systems. Thus, power control can only be toggled between ON/OFF states and would be unable to implement functions like pulse width modulation (PWM). Both DSP and PLC are relatively expensive.

The design complication and development cost of an ELC must be minimized in order to reduce the costs for installation and maintenance of the system basing on the fact that this unit is to be deployed for rural interior communities. Therefore, this paper presents the design of a simple and yet economical digital ELC system, which was developed using a modern microcontroller board. The formulation of algorithm and the hardware implementation of the ELC are presented.

During the setting of PID control based algorithm, there is no clear information on setting the value for the variable time interval. In order to obtain the optimal value of PID time interval, its tuning effect on the voltage regulation was investigated and presented. Lastly, the proposed ELC was tested under the application of varying loads.

## II. FORMULATION OF CONTROL ALGORITHM

Fig. 2 gives a simple view on how the developed ELC is connected to a micro-hydroelectric system. As it can be seen, the voltage regulation provided by the ELC is at the output terminals of the generator. The ELC consists mainly of a voltage sensor, a microcontroller unit (MCU), a phase control circuit, and a dump load. It operates by monitoring the output voltage ( $V_{out}$ ) using the voltage sensor and controlling the current to the dump load using the phase control circuit. As illustrated in Fig. 3, whenever the ELC detects  $V_{out}$  is over the nominal voltage ( $V_{nominal}$ ) of 240V (due to a decrease in consumer load), it will increase the current (hence power) to the dump load. In contrary, it reduces the current to the dump load when it detects  $V_{out}$  is below 240V due to an increase in consumer load. This allows the total load on the generator, which is the sum of consumer load and dump load, to be equalled to full load (100% load). Thus,  $V_{out}$  is maintained at 240V since full load is always on the generator.

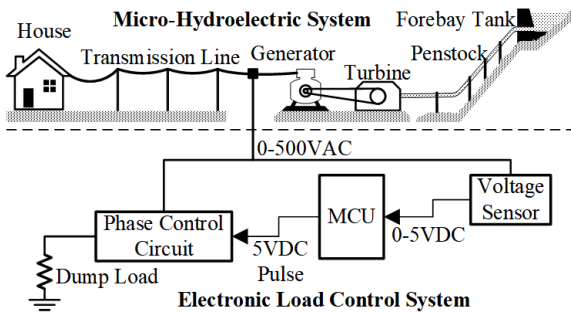


Fig. 2. Block diagram of micro-hydroelectric system attached with ELC.

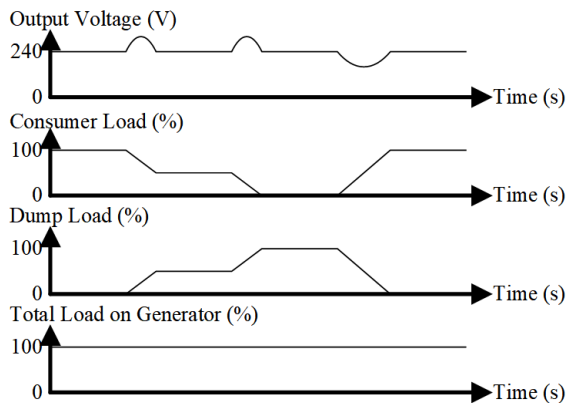


Fig. 3. Operational principal of proposed ELC.

The amount of power to the dump load is varied by adjusting the time delay ( $T_{delay}$ ) of the pulse signal to the phase control circuit. As illustrated in Fig. 4, in every half-cycle of AC voltage across the triac, the start of the time delay is applied relative to the zero-crossing events. During the time delay, the triac remains off. Once the time delay has elapsed, a voltage pulse is applied to trigger and turn on the

triac. Then, the triac conducts the remainder of the half-cycle. As a result, part of voltage (and current) is ‘chopped’ by the triac, and only a portion of input power is allowed to pass through the triac. Hence, the power to the dump load is varied.

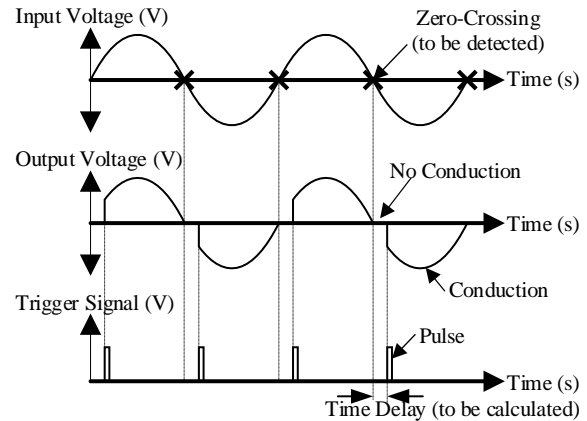


Fig. 4. Phase control waveforms.

Meanwhile, the PID control method is implemented to calculate the error, which is the deviation of  $V_{out}$  from  $V_{nominal}$ . Sequentially, it applies adjustment to the time delay using its total output ( $PID_{control\_output}$ ), which is the sum of the outputs of proportional control, integral control, and derivatives control modes. By referring to [17], the PID output can be computed by using the following equations:

$$E_{rr} = V_{ref} - V_{out} \quad (1)$$

$$P_{control\_output} = K_p \times E_{rr} \quad (2)$$

$$E_{rr\_sum} = (E_{rr\_sum} + E_{rr}) / T_{interval} \quad (3)$$

$$I_{control\_output} = K_i \times E_{rr\_sum} \quad (4)$$

$$D_{error} = (V_{out} + V_{previous}) / T_{interval} \quad (5)$$

$$D_{control\_output} = K_d \times D_{error} \quad (6)$$

$$PID_{control\_output} = P_{control\_output} + I_{control\_output} + D_{control\_output} \quad (7)$$

where  $E_{rr}$  is the error,  $E_{rr\_sum}$  is the accumulation of error,  $D_{error}$  is the derivation of error,  $P_{control\_output}$  is the output of proportional control,  $I_{control\_output}$  is the output of integral control,  $D_{control\_output}$  is output of derivative control,  $K_p$  is the proportional gain,  $K_i$  is the integral gain,  $K_d$  is the derivative gain, and  $T_{interval}$  is the time interval. As it can be seen in the equations, (1) and (2) are firstly used to obtain  $P_{control\_output}$ . Then,  $I_{control\_output}$  is obtained by using (3) and (4). Meanwhile, (5) and (6) are used to calculate  $D_{control\_output}$ . Once  $PID_{control\_output}$  is obtained, its value is used to compute  $T_{delay}$ . In order to improve on the speed response of the algorithm, the range of  $T_{delay}$  is divided into a number of sample ( $N_{sample}$ ) with a sample time ( $T_{sample}$ ). Thus, the computation of  $T_{delay}$  is expressed as:

$$N_{sample} = N_{total} - PID_{control\_output} \quad (8)$$

$$T_{delay} = N_{sample} \times T_{sample} \quad (9)$$

where  $N_{total}$  is the total sample.

Based on the operational concept, phase control, and PID control, a control algorithm is conceptualised and implemented in the ELC. Fig. 5 shows the flow chart of the control algorithm. The algorithm begins by obtaining the value of current time ( $T_{current}$ ) from the Arduino internal clock.

Then, the time change ( $T_{change}$ ) is computed from the difference in  $T_{current}$  and the previous time ( $T_{previous}$ ) and is compared with the value of time interval ( $T_{interval}$ ).

The algorithm only initiates the computation of  $T_{delay}$  if  $T_{change}$  is equal to or greater than  $T_{interval}$ . This ensures the  $V_{out}$  is constantly read and responded at a fixed time interval. The computation of  $T_{delay}$  is initiated by measuring  $V_{out}$  from the DC output of voltage sensor through pin A0 of Arduino. The value of  $V_{out}$  is normalized to the range of  $N_{sample}$ , which is from zero to total sample ( $N_{total}$ ). Sequentially,  $PID_{control\_output}$  is evaluated through (1) to (7). It is noted that the values of  $I_{control\_output}$  and  $PID_{control\_output}$  are constrained or bounded to the range of  $N_{sample}$ . The  $T_{delay}$  is applied only when a 5V pulse (interrupt signal) is received from the zero-crossing detection circuit through pin 2 (used as interrupt pin), as illustrated in Fig. 4. This allows the synchronization of the start of  $T_{delay}$  with the zero-crossing events of AC voltage. Subsequently, once  $T_{delay}$  is elapsed, a 5V pulse is output to pin 3 to turn on the triac. The 5V pulse to the triac only last for 10 $\mu$ s in order to put the triac back to off state for the next zero-crossing event. Then, the algorithm loops back to its beginning.

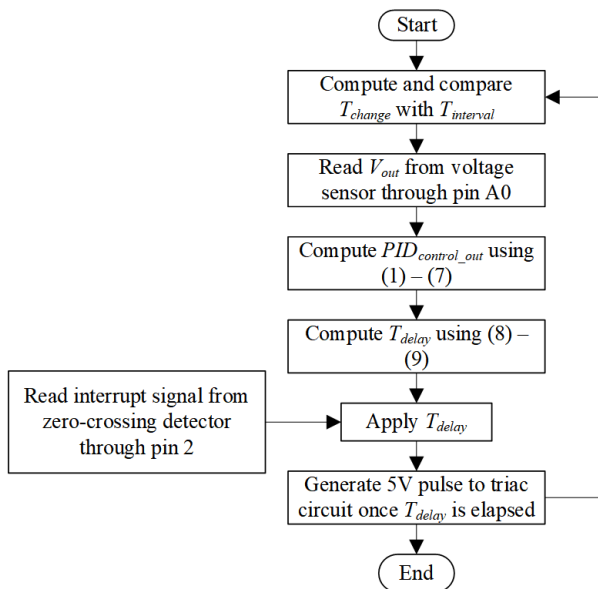


Fig. 5. Flow chart of algorithm.

### III. HARDWARE IMPLEMENTATION

The following two parameters are considered for calculating or selecting the ratings of components used in the design of the ELC:

- The maximum power generated by generator.
- The maximum generator output voltage under no load condition.

The ELC in this paper is prototyped to handle a generator with a maximum power of 5kW and a maximum output voltage of 500VAC.

Fig. 6 shows the schematic diagram of the ELC designed in this research. It consists of a double 240VAC-12/24VDC voltage converter module, a voltage transducer TEC-AU1C5 module, an Arduino UNO board, a phase control based power control circuit, and a 5kW dump load. The voltage converter is linked to the main transmission line and

converts 240VAC into 12VDC and 24VDC for powering the Arduino board and voltage transducer, respectively. Similarly, the voltage transducer also linked to the main transmission line, and it converts the AC output voltage (0V – 500V) into a corresponding DC voltage (0V – 5V), which is sent to the analogue pin A0 of the Arduino board. The Arduino board also executes the control algorithm and generates trigger signals to the phase control circuit through its digital pin D3. Meanwhile, the phase control circuit functions to control the amount of power delivered to the dump load, and it is a combination of a zero-crossing detection circuit and a triac circuit (triac and driver circuit).

The zero-crossing detection circuit generates a pulse signal for every time the AC voltage crosses the zero volts, and the signal is sent to the digital pin D2 of the Arduino board for synchronising the trigger signal with zero-crossing event. The circuit consists of a bi-directional input optically coupled isolator H11AA1 and three resistors. A 10k $\Omega$  resistor (labelled R1) is used as a pull-up resistor. Meanwhile, two 15k $\Omega$  resistors (labelled R2 and R3) are used as current limiting resistors, which restrict the current into the light emitting diodes (LEDs) inside the isolator to be 15.9mA.

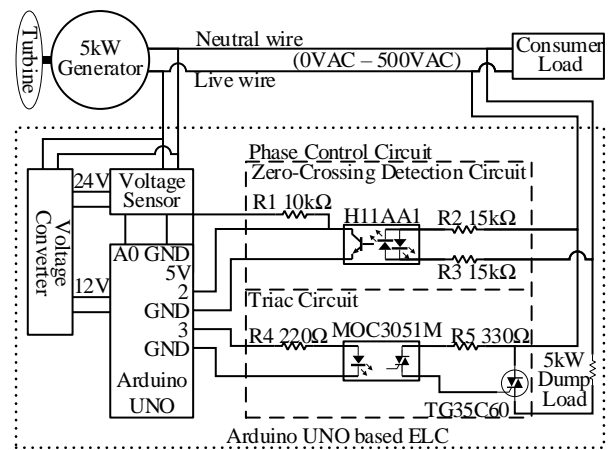


Fig. 6. Schematic diagram of Arduino UNO based ELC.

The triac is responsible for chopping the AC voltage (and current) in every half-cycle. The voltage and current ratings of the triac is selected according to the two parameters mentioned earlier. The 5kW power will require the triac to handle a current up to 20A at 240VAC. Therefore, based on the commercially available rating, a triac (TG35C60) with 600V, 35A is used.

Meanwhile, the triac driver circuit is used to amplify the low-power trigger signal from the Arduino and provide isolation between the low-power Arduino and the high-power triac for safety. It is made of a random-phase optocoupler MOC3051M and two current limiting resistors. A 330 $\Omega$  resistor labelled R4 is used to set the current into the LED to be less than 15mA. Meanwhile, a 1.5k  $\Omega$  resistor labelled R5 is used to limit the current into the right side of the optocoupler to be less than 1A. Lastly, a dump load is used to consume the excess power resulted from a disconnected consumer load. It must have same or more than the power rating of the generator in order consume all the power during no load condition.



It can be any resistive loads like light bulbs, water heaters, and air heaters.

IV. LABORATORY SETUP

Both the ELC circuit and the algorithm were tested experimentally by using the setup as shown in the block diagram in Fig. 7.

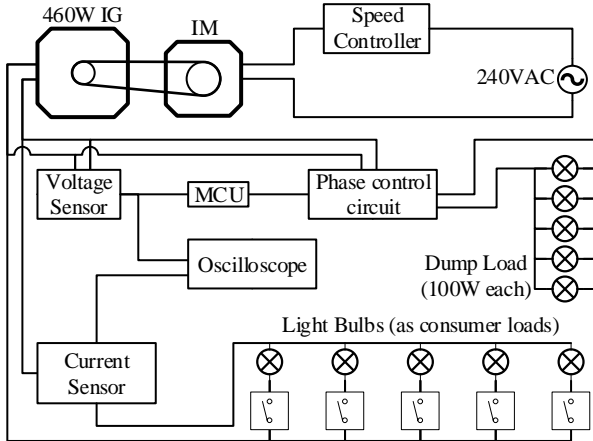


Fig. 7. Laboratory setup.

In the experimental setup, an induction motor (IM) and a 460W/80Hz induction generator (IG) were used to mimic the operation of a micro-hydroelectric system. The speed of the IM was controlled by a motor speed controller. A set of five 100W light bulbs was used to form a 500W dump load. Light bulbs with different power ratings were also used to simulate the load variations. An oscilloscope was used to obtain the waveforms of  $V_{out}$  during tests. The waveforms were later analysed by using LabVIEW SignalExpress Tektronix Edition software. Furthermore, a current sensor (TEC-AI1B1) was used in order for the oscilloscope to record the change in the total current of consumer load ( $I_{t\_consumer}$ ).

V. RESULTS AND DISCUSSION

The tuning effect of  $T_{interval}$  on the response of  $V_{out}$  was investigated by firstly obtaining three sets of PID gains ( $K_p$ ,  $K_i$ , and  $K_d$ ) that were tuned under three different values of  $T_{interval}$ : 5ms, 10ms, 30ms. It is noted that fast response was assumed to be the ideal response of the ELC in this investigation. Hence, every set of PID gains was tuned to obtain fast voltage regulation. Table I shows the optimal values of the PID gains obtained under different value of  $T_{interval}$ . The data in the table clearly shows that the optimal values of the PID gains will be different when they are tuned under different  $T_{interval}$ . Then, the ELC regulated  $V_{out}$  from 354VAC to nearly 240VAC using the three sets of PID gains, separately. The resulted three  $V_{out}$  waveforms were recorded by using an oscilloscope, and they are shown in Fig. 8. Later, the rise time ( $T_{rise}$ ), percentage of overshoot (PO), settling time ( $T_{settling}$ ), and steady-state error ( $E_{ss}$ ) of the waveforms were measured using the LabView SignalExpress Tektronix Edition software. These four waveform characteristics were used to analyse the tuning effect of  $T_{interval}$ , and they are presented in Table II. A good response of a system controlled by PID control should have

the waveform characteristics to be minimized. However, the results showed that the increase in  $T_{interval}$  causes negative effects to  $T_{rise}$ ,  $T_{settling}$ , and  $E_{ss}$  by increasing their values. Meanwhile, the change in PO was inconsistent, but the values of PO at  $T_{interval} = 5ms$  and 30ms are not much different. Therefore, the value of  $T_{interval}$  should be set to its minimum value in order to minimize the values of  $T_{rise}$ , PO,  $T_{settling}$ , and  $E_{ss}$ . In this research, 5ms is the minimum value of  $T_{interval}$  as the Arduino UNO running at 16Mhz allowed one loop of the algorithms to be completed below that times. The minimum value of  $T_{interval}$  will be different when different microcontrollers with different processing speeds are used.

Table I: Optimal values of PID gains for different  $T_{interval}$ .

Time Interval, $T_{interval}$ (ms)	Proportional Gain, $K_p$	Integral Gain, $K_i$	Derivative Gain, $K_d$
5	2	0.8	5
10	2	3	10
30	1.3	20	20

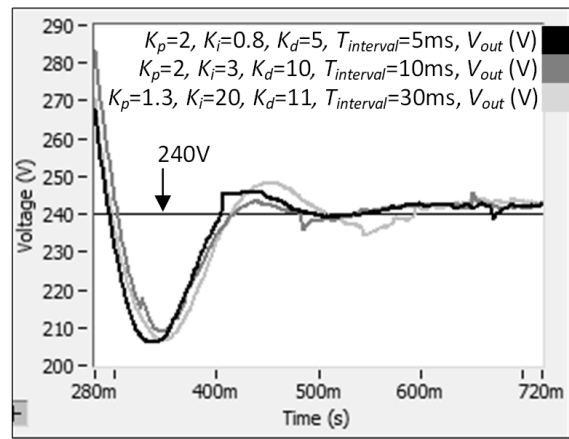


Fig. 8. Transient waveforms of  $V_{out}$  for  $T_{interval}$  tuning.

Table II: Tuning effect of  $T_{interval}$ .

Time Interval, $T_{interval}$ (ms)	Rise Time, $T_{rise}$ (ms)	Percentage of Overshoot, PO (%)	Settling Time, $T_{settling}$ (ms)	Steady-State Error, $E_{ss}$ (V)
5	42.21	14.90	353	2.34
10	43.29	13.80	368	2.38
30	43.93	14.88	562	2.68

Next, by setting  $K_p = 2$ ,  $K_i = 0.8$ ,  $K_d = 5$ , and  $T_{interval}$  to 5ms, the developed ELC was tested under load variations. Fig. 9 shows the  $V_{out}$  regulation by the ELC with increasing consumer loads. As it can be seen, initially at 0s, the ELC regulated  $V_{out}$  nearly at 240V under zero consumer load condition whereby the total current of consumer load ( $I_{t\_consumer}$ ) is 0A. At this moment, all the generated power was absorbed by the dump load. After 1s, the increase of  $I_{t\_consumer}$  to 0.06A showed a 15W consumer load was switched on. This load change caused  $V_{out}$  to have a 1.8% negative overshoot, which indicated the generator was overloaded. Same thing happened when another 15W load was turned on and  $I_{t\_consumer}$  was doubled to 0.12A after 3s.

The ELC responded by releasing similar amount of power from the dump load and regulated  $V_{out}$  to 240V with a settling time of 333ms for the two load changes. Sequentially, an increment of 0.17A to  $I_{t\_consumer}$  after 5s and 7s showed that two separate 40W consumer loads were added to the generator. The last added consumer load was a 60W load consuming 0.25A. The 40W and 60W load changes caused the respective 2.8% and 3.9% negative overshoots. Despite that, the ELC maintained  $V_{out}$  at 240V, and the settling times of  $V_{out}$  for the 40W and 60W load changes were 556ms and 828ms, respectively. From here, it can be concluded that the overshoot and settling time change correspondingly to the size of the load. This statement also applied to  $V_{out}$  during decreasing consumer load, as shown in Fig. 10. The disconnections of 60W, 40W, and 15W loads caused 2.9%, 1.7%, and 1.1% overshoots, respectively, and their respective settling times were 720ms, 464ms, and 272ms. The only difference is that the overshoot is in positive direction. This is because the loss of consumer load caused the generator to speed up and  $V_{out}$  to increase. In reality, the consumer load consumption is no consistent. Hence, the ELC was later tested with random consumer load connection and disconnection. The Obtained waveform is as shown in Fig. 11. Initially, a total of 100W consumer loads already connected to the generator. Then, another 15W load was added after 1s. Subsequently, 60W and 40W loads were removed sequentially after 4s and 6s. Lastly, the 60W load was reconnected to the generator. Nevertheless,  $V_{out}$  was able to be maintained to 240V despite the load changes. Therefore, the overall results proved that the developed ELC circuit and algorithm was able to regulate  $V_{out}$  of a micro-hydroelectric system. Even though the ELC was tested experimentally using the 460W generator, it is applicable for any micro-hydroelectric system with a power rating up to 5kW.

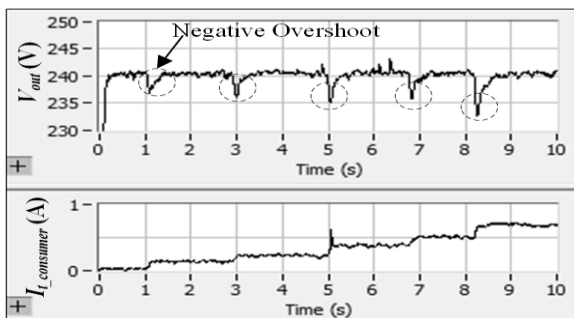


Fig. 9.  $V_{out}$  and  $I_{t\_consumer}$  waveforms for increasing consumer load.

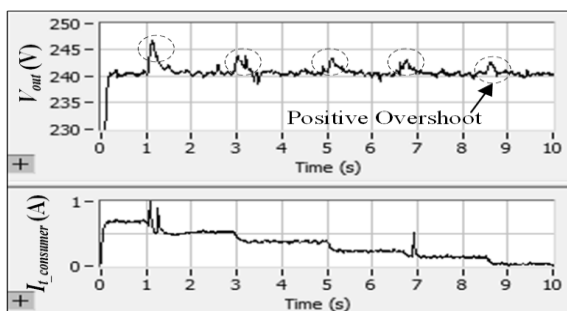


Fig. 10.  $V_{out}$  and  $I_{t\_consumer}$  waveforms for decreasing consumer load.

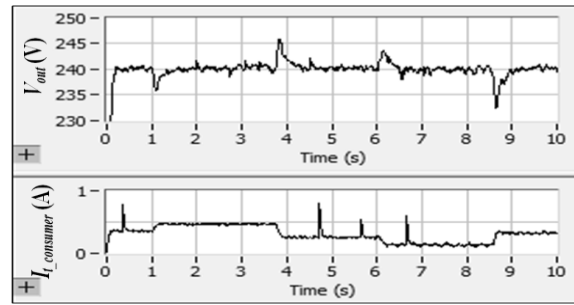


Fig. 11.  $V_{out}$  and  $I_{t\_consumer}$  waveforms for random consumer load consumption.

## VI. CONCLUSION

The concept of the digitally controlled ELC proposed in this paper is simple and cost-effective to be fabricated for the voltage regulation of the micro-hydroelectric system. The developed ELC circuit is no complex, and it consists mainly of a voltage sensor, a microcontroller board (loaded with the PID control based algorithm), a phase control based power electronic circuit, and a dump load. Moreover, the control algorithm of the ELC was formulated and implemented without involving the complicated mathematical modelling of the micro-hydroelectric system. On the other hand, the investigation on the tuning effect of time interval on the voltage regulation showed that the increase of time interval tends to cause the rise time, settling time, and steady-state error of the output voltage to increase. Hence, the value of the time interval should be set to its minimum value. Meanwhile, during the load variation tests, all the voltage fluctuations caused by the applications and removals of loads were completely regulated by the ELC to nearly 240V, and this proved that the ELC design proposed in this paper is applicable for the voltage regulation of the micro-hydroelectric system.

## ACKNOWLEDGMENT

The authors would like to thank Universiti Malaysia Sarawak (UNIMAS) for the research facilities provided. In addition, the authors also thank the technicians from Department of Electrical and Electronic Engineering (Faculty of Engineering, UNIMAS) for their assistance.

## REFERENCES

1. R.R. Singh, T. R. Chelliah, and P. Agarwal, "Power electronics in hydro electric energy systems – A review", *Renewable and Sustainable Energy Reviews* 32, 2014, pp. 944–959.
2. M. Amran, M. Radzi, M. Lqbal, and A. Hakim, "Basic design aspects of micro hydro power plant and its potential development in Malaysia", *PECon 2004. Proceedings. National Power and Energy Conference*, 2004, pp. 220–223.
3. S. Pokhrel, P. Parajuli, and B. Adhikary, "Design and performance of lab fabricated induction generator controller", *2nd International Conference on the Developments in Renewable Energy Technology (ICDRET 2012)*, 2012, pp. 1–3.
4. S. S. Murthy, G. Bhuvaneshwari, S. Gao, and M. S. L. Gayathri, "Performance Analysis of a Self Excited Induction Generator with Digitally Controlled Electronic Load Controller for Micro Hydrel Power Generation", *2008 Joint International Conference on Power System Technology and IEEE Power India Conference*, 2008, pp. 1–6.

5. S. Gao, G. Bhuvanewari, S. S. Murthy, and U. Kalla, "Efficient voltage regulation scheme for three-phase self-excited induction generator feeding single-phase load in remote locations", *IET Renewable Power Generation* 8(2), 2014, pp.100–108.
6. B. Singh, V. Rajagopal, A. Chandra, and K. Al-Haddad, "Development of electronic load controller for IAG based standalone hydro power generation", *2010 Annual IEEE India Conference (INDICON)*, 2010, pp. 1–4.
7. V. Rajagopal and B. Singh, "Improved electronic load controller for offgrid induction generator in small hydro power generation", *India International Conference on Power Electronics 2010 (IICPE2010)*, 2011, pp. 1–7.
8. B. Singh and V. Rajagopal, "Neural-network-based integrated electronic load controller for isolated asynchronous generators in small hydro generation", *IEEE Transactions on Industrial Electronics* 58(9), 2011, pp. 4264–4274.
9. V. Rajagopal, B. Singh, and G. K. Kasal, "Electronic load controller with power quality improvement of isolated induction generator for small hydro power generation", *IET Renewable Power Generation* 5(2), 2011, pp. 202–213.
10. G. Chetana, S. K. Shah, and S. J. Patel, "Analysis and design of electronic load controller using FLC for self excited induction generator", *2012 1st International Conference on Emerging Technology Trends in Electronics, Communication & Networking*, 2012, pp. 1–7.
11. B. Singh and V. Rajagopal, "Digital control of voltage and frequency of induction generator in isolated small hydro system", *2012 IEEE International Conference on Power Electronics, Drives and Energy Systems (PEDES)*, 2012, pp. 1–7.
12. R. R. Chilipi, B. Singh, S. S. Murthy, S. Madishetti, and G. Bhuvanewari, "Design and implementation of dynamic electronic load controller for three-phase self-excited induction generator in remote small-hydro power generation", *IET Renewable Power Generation* 8(3), 2014, pp. 269–280.
13. U. K. Kalla, B. Singh, and S. S. Murthy, "Normalised adaptive linear element-based control of single-phase self excited induction generator feeding fluctuating loads", *IET Power Electronics* 7(8), 2014, pp. 2151–2160.
14. V. Rajagopal and B. Singh, "Electronic load controller using IcosΦ algorithm for standalone induction generator", *2010 Joint International Conference on Power Electronics, Drives and Energy Systems & 2010 Power India*, 2010, pp. 1–6.
15. D. K. Palwalia, "STATCOM based voltage and frequency regulator for self excited induction generator", *2013 International Conference on Electrical, Electronics and System Engineering (ICEESE)*, 2013, pp. 102–107.
16. M. Kabalan, D. Tamir, and P. Singh, "Electrical load controller for rural micro-hydroelectric systems using a programmable logic controller", *2015 IEEE Canada International Humanitarian Technology Conference (IHTC2015)*, 2015, pp. 1–4.
17. R. Anderson and D. Cervo, *Pro Arduino*, Apress, 2013, pp. 129–142.

Faculty of Engenering in UNIMAS. His research interests are very-large-scale integration (VLSI) and embedded digital designs.

### AUTHORS PROFILE



**Chong Yee Ming** recieved his Bachelor of Engineering (Honors) in Electronics (Computer) from Universiti Malaysia Sarawak (UNIMAS), Kota Samarahan, Malaysia in 2014. After graduated from his bachelor degree, he joined UNIMAS again to continue his Master in Engineering of Electronic Computer (Research). His reseach interest is in developing controller for regulating the fluctuating output voltage of micro-hydroelectric system.



**Martin Anyi** received his Bachelor of Engineering (Hons) in Electronics (Telecommunication) from Universiti Malaysia Sarawak (UNIMAS) and Master of Engineering in Computer and Telecommunication from Universiti Kebangsaan Malaysia (UKM), in 1997 and 2000 respectively. He is a senior lecturer of Faculty of Engenering in UNIMAS. His research interests are telecommunication, microcontroller interfacing and programming, circuit design, electrical power, renewable energy systems, power electronic and electronic control.



**Lakshmanan Gurusamy** recived both his Master of Enginnering in Microelectronics and Ph.D. in Electrical, Electronics & Systems Engineering from Univeristi Kebangsaan Malaysia (UKM). He is a senior lecturer of